Fluctuations in the Enormous Toroidal Plasma Device at UCLA

Robert Niederriter
Physics Department, Lawrence University
(Dated: September 14, 2009)

Turbulence and transport across magnetic field lines disrupt plasma confinement, which is particularly troublesome in toroidal geometries potentially useful for fusion energy. We investigate fluctuations of a helium plasma in the Enormous Toroidal Plasma Device (ETPD) at UCLA using 4-tip Langmuir probes to measure potential and ion saturation current. ETPD is a simple magnetized torus with major radius 5 m. The toroidal vacuum chamber has a rectangular cross section that is 3 m tall and 2 m wide. Plasma is generated by a lanthanum hexaboride (LaB6) cathode discharge into a helical magnetic field produced by a ~ 250 G toroidal field and a ~ 6 G vertical field. Typical plasma density is $n_e \sim 10^{13}$ cm^{-3} and typical electron temperature is $T_e \sim 10-20$ eV. Observed fluctuations are characterized and compared with theories of drift waves and interchange modes.

I. INTRODUCTION

Plasma physics since the mid 1900s has pursued magnetic confinement for fusion energy. Primary difficulties in magnetic confinement devices arise from instabilities in the plasma that increase transport across magnetic field lines and reduce confinement.

Here we investigate fluctuations in the Enormous Toroidal Plasma Device at UCLA. This basic plasma science device operates at much lower temperature and density scales than the modern fusion devices, allowing more detailed probe measurements to be made. Many of the same fluctuations and instabilities that plague the larger devices only depend on dimensionless quantities and ratios, and so they can still be observed in experiments at lower temperature and density scales. Characterizing these fluctuations may help solve the confinement problems in similar devices.

II. APPARATUS

The research was done using the Enormous Toroidal Plasma Device (ETPD) at the Basic Plasma Science Facility at the University of California, Los Angeles.

A. The Enormous Toroidal Plasma Device

Figure 1 shows the device itself, consisting of a toroidal vacuum chamber with major radius 10 meters and rectangular cross section: 2 meters horizontally by 3 meters vertically. The plasma chamber maintains a dynamic vacuum in the range $1-4$ mTorr. Five turbo molecular and mechanical pump pairs run continuously as gases are fed in at rates controlled by a mass-flow controller. Setting the inward gas flow rate controls the pressure inside the device. Gases used are hydrogen, helium, neon, and argon, with the option of mixing gases. The red coils in the figure provide toroidal magnetic fields up to 250 gauss. The blue coils provide vertical magnetic fields of ~ 6 gauss so the total magnetic field is helical. Plentiful ball valves and windows provide access for probing the plasma.

FIG. 1: The Enormous Toroidal Plasma Device, described in the text.

Plasma is produced by pulsed discharge from a lanthinum hexaboride (LaB_6) cathode. Four 10 cm x 10 cm plates of lanthinum hexaboride are heated from behind by a thick graphite coil. Heating the LaB_6 cathode to ~ 2000 K allows electrons in the cathode material to escape. The freed electrons are accelerated across 380 V in 45 cm, through a wire mesh that passes 70% of the electrons. These fast electrons follow the helical field lines, exciting the gas in the plasma chamber.

B. Langmuir Probes

Single-tip Langmuir probes were used extensively in initial diagnostics of the plasma parameters and for obtaining two-probe phase information.

A four-tip Langmuir probe was used for simultaneous measurements of floating potential and ion saturation current. The four tips are arranged in a diamond pattern. The two vertically separated tips collect floating potential (V_f) with a tip spacing of 3 millimeters. The two horizontally separated tips are separated by 3 millimeters and biased 135 volts relative to each other, allowing measurement of differential ion saturation current (I_{sat}) between the tips. Differential set up ensures the negatively biased probe tip is sufficiently negative to collect I_{sat} and removes the danger of collecting very high electron saturation currents. This probe design allows the simultaneous measurement of plasma density and floating potential for characterization of plasma fluctuations. I_{sat} is proportional to the plasma density, which can be derived from the signal if the temperature is known.

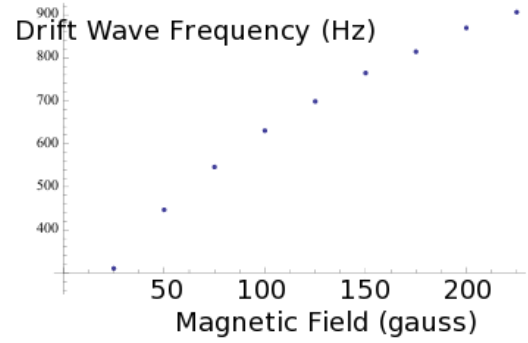

FIG. 2: Numerical finite-difference solutions for various toroidal magnetic fields. The points represent the fastest growing modes for each magnetic field.

III. PLASMA INSTABILITIES

Instabilities can arise in a plasma which possesses sources of free energy, that is plasmas that are not in global thermodynamic equilibrium. Natural, industrial, and laboratory plasma sources all tend to form plasmas with density and temperature gradients, and often there are also electric and magnetic fields involved. These conditions of non-equilibrium spawn instabilities in the plasma.

Plasma instabilities are commonly observed in laboratory plasmas as well as in natural plasmas and those for industrial use. Of particular interest, plasma devices designed for nuclear fusion exhibit large amounts of turbulence; these devices rely strongly on confinement for function and survival, and large turbulent structures can be extremely destructive. Common instabilities found in toroidal devices are drift waves and interchange modes, which thrive on the density gradients and magnetic field gradients common to these geometries.

A. Drift Waves

Drift waves are formed on the density gradients of a plasma, driven by the non-uniform pressure. Small perturbations in density and potential are propelled by the $\vec{\boldsymbol{E}} \times \vec{\boldsymbol{B}}$ drift.

Drift wave linear theory can be helpful in predicting the frequency of waves we may see in the Enormous Toroidal Plasma Device. A fluid model of a plasma can be used to investigate the linear properties of the drift waves instability. We have employed an analytic model using density continuity, momentum continuity, and current continuity equations:

$$0 = \frac{\partial n}{\partial t} + \boldsymbol{\nabla} \cdot (n\boldsymbol{v_e}) \tag{1}$$

$$nm_e \frac{d\boldsymbol{v_e}}{dt} = -\boldsymbol{\nabla} p - ne\left(\boldsymbol{E} + \frac{1}{c}\boldsymbol{v_e} \times \boldsymbol{E}\right) - nm_e\nu_{ei}\left(\boldsymbol{v_e} - \boldsymbol{v_i}\right) - nm_e\nu_{en}\boldsymbol{v_e} \tag{2}$$

$$0 = \boldsymbol{\nabla} \cdot \boldsymbol{J} \tag{3}$$

Assuming oscillatory solutions of the form $f(x) = f(r)\exp(im\theta + ik_{\parallel}z - i\omega t)$, we obtain a single second-order differential equation for the electric potential: an eigenvalue equation for the oscillation frequency. Solving this equation by a finite-difference method using Mathematica yields a prediction for the frequency of drift wave oscillations. Solutions are complex quantities: the real part is the fluctuation frequency, and the imaginary part is the growth rate for fluctuations of that frequency. There are in general many solutions to the equation, but we consider only the fastest growing solution as the dominant mode of oscillation. Using experimentally measured profiles, we have solved these equations for drift-wave stability in ETPD. The results are shown in Figure 2, showing unstable drift-modes should be expected.

These equations do not take into account the curvature of the magnetic field lines, or the radial gradient in the magnetic field. Adding this to the model would enable the growth of interchange modes.

B. Interchange

Similar to drift waves, interchange instabilities derive their free energy from pressure gradients in the plasma. However, interchange modes are driven by forces associated with non-uniform magnetic fields. Interchange instabilities are exactly what their name implies: high density plasma is exchanged with lower density plasma. If all other conditions are constant, the exchange does not change the free energy of the system. In a plasma with a non-uniform magnetic field, there are regions of higher

and lower magnetic fields. Exchanging a dense plasma from a region of higher magnetic field with less dense plasma from a region of lower magnetic field lowers the free energy of the system.

A common analogy to interchange is a dense fluid at rest on a less dense fluid. Gravity pulls stronger on the more dense fluid, so the system's equilibrium would put the more dense fluid below the less dense fluid. A small perturbation in the boundary between the two fluids can be thought of as an exchange between a region of more dense fluid and a region of less dense fluid. Moving a small section of the more dense fluid down and moving the same volume of less dense fluid up to take its place reduces the energy of the system toward equilibrium. This is the well known Raleigh-Taylor instability.

In toroidal devices, the toroidal magnetic field decreases proportional to $1/r$ towards the outside of the device. Interchange instabilities depend on a magnetic field gradient in the same direction as the pressure gradient. Therefore these fluctuations are only expected to be present on the outboard, or low-field, side of a toroidal plasma. This is in contrast to simple drift waves, which are expected to be excited wherever pressure gradients exist.

IV. RESULTS

We are interested in fluctuations in the plasma density, and we approximate density fluctuations by I_{sat} fluctuations measured with Langmuir probes. I_{sat} fluctuations might represent waves and turbulence in the plasma. To analyze fluctuations, I_{sat} signals are decomposed into frequency-space elements using fast fourier transforms (FFT). The power spectrum of a signal is the squared absolute value of the the FFT. The cross spectrum of two signals is the product of the FFT of one signal with the complex conjugate of the FFT of the other signal. The cross phase of two signals is the arctangent of the quotient of the imaginary and real parts of the cross spectrum.

A simple test to discriminate between the interchange and drift wave drive is the spatial pattern of the fluctuations: interchange modes would be expected only on the outboard side. Transport driven by these modes would therefore be localized to the outboard side and asymmetric density profiles might result, e.g. with a broader density profile on the outboard as compared to the inboard side.

By changing the neutral-fill pressure in the plasma device, we observe a progression in plasma cross secions as shown in Figure 3. The absolute densities in each case are not identical; the present study only concerns the relative density cross secinos, approximated using I_{sat} measurements over locations in a plane. In all cases, the density decreases away from the center of the plasma column. The density decreases more quickly in some directions than in others, however, and these density gradients

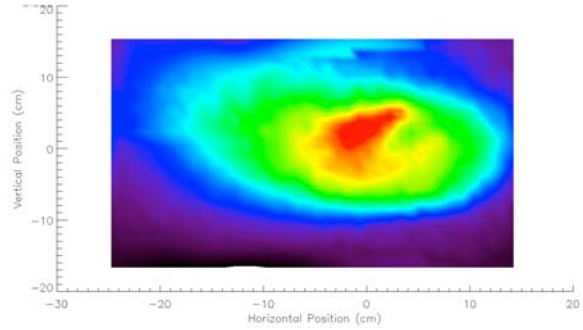

(a)1.1 mTorr

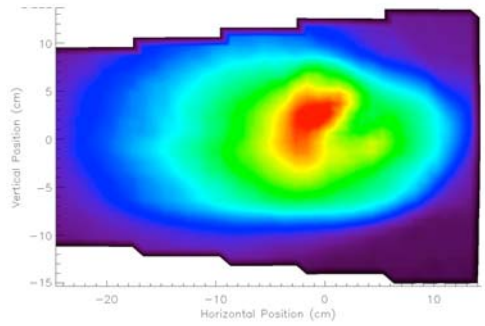

(b)1.4 mTorr

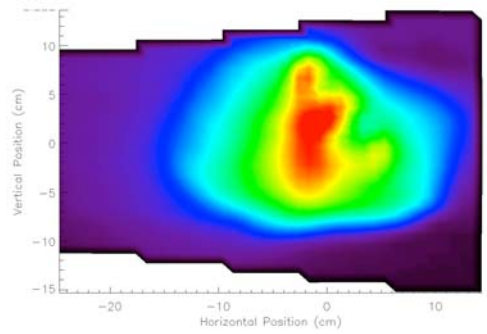

(c)1.7 mTorr

FIG. 3: Approximate, relative plasma density for various neutral-fill pressures. Density is approximated from I_{sat} mesurements at 41 radial locations at each of 17 angular locations. Each plane is normalized to its own maximum value to show relative density only. The axes are horizontal and vertical position, measured horizontally from the center of the plasma chamber and vertically from the vertical probe drive's zero position with positive directions toward the inboard side of the torus and up (zero vertical position is arbitrary, but near to the center of the plasma column).

change with neutral-fill pressure. On the outboard side of the plasma column the density decreases less quickly than on the inboard side, top, and bottom of the plasma column. The density cross section is not a simple circular shape, but stretched toward the outboard side. This effect is diminished in the higher pressure cases, and the plasma column approaches a circular shape at 1.7 mTorr.

Integrating the I_{sat} power spectrum over a frequency range, we can investigate the spatial dependence of fluc-

tuations. The data in Figures 4 and 5 were taken on a line approximately through the center of the plasma column to give spatial dependence of fluctuations. The zero of the spatial scale is set as the center of the plasma chamber, which is roughly the center of the plasma column. Positive position is the inboard side of the plasma column, towards the center of the torus. Negative position is the outboard side of the plasma column, towards the outside of the torus.

A complication encountered with the apparatus results in consistent, extraneous signals in all of the plasma diagnostics. FFTs show waves at harmonics of 360 Hz that appear as 360 Hz sawtooth waves on the oscilloscope. We have tested various possible sources of 360 Hz interference, and we have traced it back to the cathode heater power supply. The power supply operates from 3-phase power and generates a high voltage DC supply with 360 Hz ripples on top. The coupling mechanism between the heater supply and the plasma is unknown; the heater is inside the plasma chamber, and is probably surrounded by plasma. This could couple to the cathode discharge or to some other aspect of the plasma. These signals at 360 Hz (and 720 Hz, etc) obscure any low frequency fluctuations that might occur in the plasma, so we limit our analysis to frequency ranges above 1 kHz.

Spatial features of the plasma can be reconstructed by moving a Langmuir probe on a line horizontally through the plasma. At each position, 10 plasma pulses were recorded. Figures 4 5 show where in the plasma column fluctuations in different frequency ranges appear. The power spectra change considerably near 10 kHz, prompting us to sum over the two ranges separately: 1-10 kHz and 10-300 kHz. Below 1 kHz, the power spectra are all dominated by harmonics of 360 Hz due to some interference from the apparatus, and not likely interesting physically. 300 kHz is a somewhat arbitrary cut-off. Beyond 300 kHz, the power spectra simply become too weak to be significant.

Looking at the I_{sat} profiles, shown in blue, we can see a progression from a fuzzy, wide plasma column at 1.1 mTorr to a sharp, narrow plasma column at 1.7 mTorr.

For all six cases of different pressure and frequency range, there are more or stronger fluctuations on the outboard side of the plasma than on the inboard side. The fluctuations in both ranges at 1.1 mTorr are broadly localized in space, and there is much more spatial variation in the fluctuation profile at this lower pressure than at the higher pressures. This is similar to how the plasma profile at low pressure seems fuzzy and wide compared to the profile at higher pressure.

The fluctuation profiles for the two frequency ranges at 1.4 mTorr appear quite different. The low frequency range shows much of the power narrowly concentrated in the center of the plasma, with The high frequency range shows the power concetrated mostly on the outboard side of the plasma column.

The relative amplitudes of the maximum high- and low-frequency fluctuations are different for each pressure.

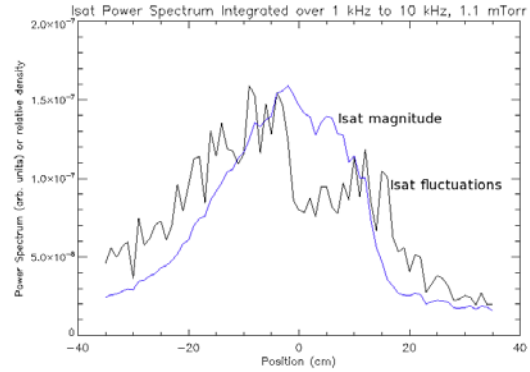

(a)1.1 mTorr

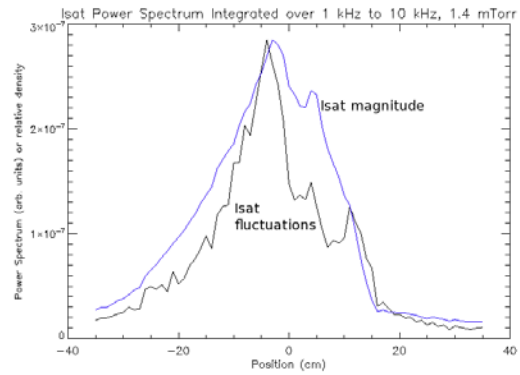

(b)1.4 mTorr

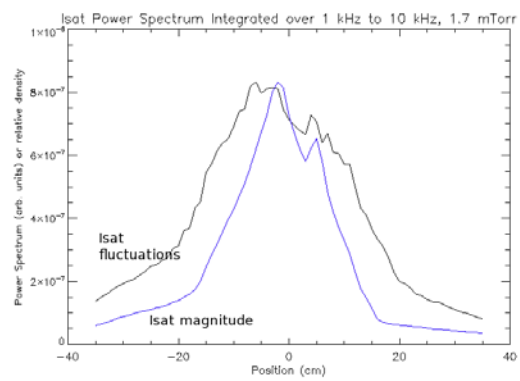

(c)1.7 mTorr

FIG. 4: I_{sat} fluctuations power spectrum summed over 10 kHz to 300 kHz as a function of position. I_{sat} profile ($\sim$ density) shown in blue for spatial comparison.

At 1.1 mTorr, max low-frequency fluctuations are about twice as large as max high-frequency fluctuations. At 1.4 mTorr, high- and low-frequency flucuations are nearly the same amplitude. At 1.7 mTorr, high-frequency fluctuations are about four times larger than low-frequency fluctuations.

We can also examine the phase relationship between the I_{sat} fluctuations for two spatially separated Langmuir probes. The phase may provide information about the poloidal mode number of plasma fluctuations. One Langmuir probe is held stationary to use as reference

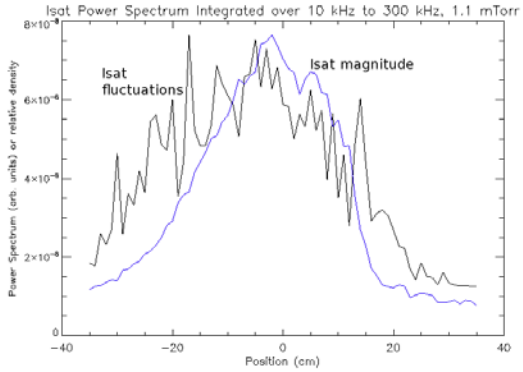

(a)1.1 mTorr

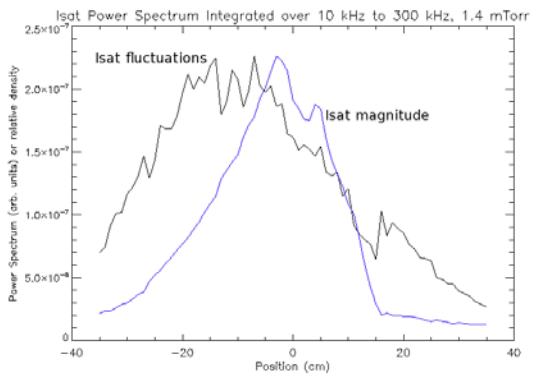

(b)1.4 mTorr

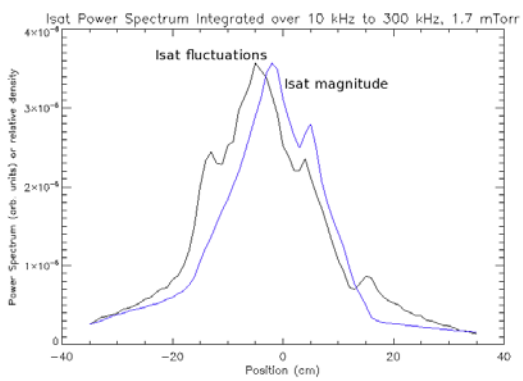

(c)1.7 mTorr

FIG. 5: I_{sat} fluctuations power spectrum summed over 10 kHz to 300 kHz as a function of position. I_{sat} profile ($\sim$ density) shown in blue for spatial comparison.

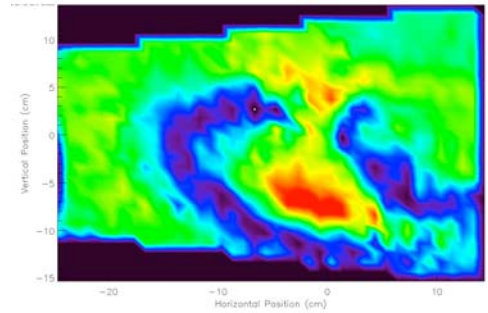

(a)1.1 mTorr

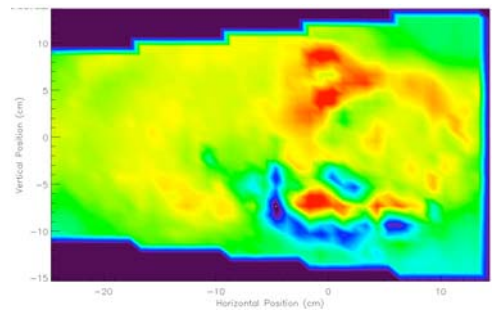

(b)1.4 mTorr

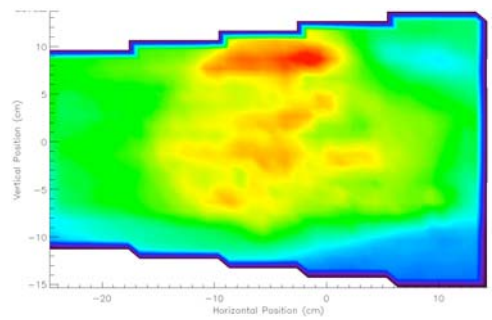

(c)1.7 mTorr

FIG. 6: Cross-phase between I_{sat} fluctuations for two Langmuir probes, calculated from cross-spectrum summed over 1 kHz to 10 kHz. Plots are cosine of the phase angle, so that negative and positive angles are identical; the cosine value is weighted by the rms I_{sat} fluctuations over 1 kHz to 10 kHz measured by the moving probe. Red represents in-phase, and blue/purple represents out of phase. One probe is held stationary at approximately $x = -5$, $y = 0$, while the other is moved throughout the plasma to the positions indicated.

while another probe is moved through a cross section of the plasma column. The probes were seperated by about one meter along the toroidal direction of the plasma.

The phase is calculated using the cross spectrum summed over a range of frequencies 1 to 10 kHz. The low sampling rate used for these cross sections makes higher frequencies unreliable. The phase angle is arctangent of the quotient of the imaginary and real parts of the summed cross spectrum. The plots shown in Figure 6 are the cosine of the phase angle weighted at each location by the rms I_{sat} fluctuations within the same frequency band. Locations where the two probes are in phase appear red, and out of phase regions appear green or blue.

Focusing on a case with the lowest neutral-fill pressure possible on the apparatus, 0.9 mTorr, we vary the toroidal magnetic field to observe how the frequency of fluctuations responds. The vertical field was also adjusted proportionally so that the plasma column stayed in the same position for all of the fields. Data was taken by two methods: in lines of 21 locations spaced horizontally across the plasma with 10 repititions per location, and at a single location with 50 repititions. Averaging the I_{sat} power spectrum across all positions to combine

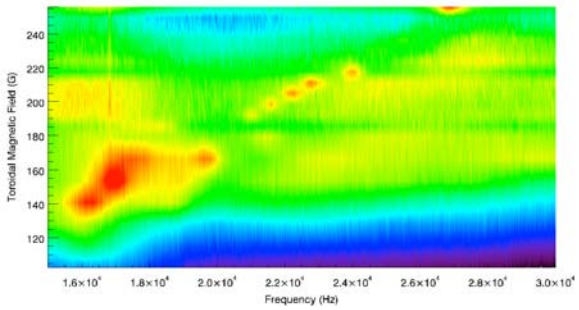

FIG. 7: I_{sat} power spectrum vs frequency and toroidal magnetic field for low neutral pressure (0.9 mTorr). Data taken at a single location with 50 shots for various magnetic field settings, 800, 900, 1000, 1100, 1200, 1400, 1700, 2000 and also over a line of 21 locations on the outboard side of the plasma at 10 shots/location for various magnetic field settings. The power spectra were averaged for all points along the lines and plotted alongside the averaged power spectra from the single locations. The averaging accounts for the different numbers of shots recorded at each magnetic field value.

the data taken in lines with those taken at a single point. Combining the power spectra for the various magnetic fields into a single array, we get the power spectrum as a function of frequency and toroidal magnetic field shown in Figure 7.

Waves appear as frequency bands with relatively high energy: red or orange on the plot. We can see the response of fluctuations to varied toroidal magnetic field. For one such fluctuation, the frequency increases as toroidal magnetic field increases.

V. DISCUSSION

The change in density cross sections and profiles with neutral-fill pressure may indicate a transition in the transport across magnetic field lines. The narrow profile at 1.7 mTorr implies less outboard-directed transport than do the broad profiles and elongated, fuzzy cross sections at 1.1 and 1.4 mTorr. In each case, the cathode discharge acts on a roughly 20 cm x 20 cm square cross section, but the measured plasma shape varies with neutral-fill pressure.

The consistent concentration of fluctuations on the outboard side of the plasma column suggests active interchange instabilities. Interchange instabilities drive plasma outward and are often involved in transport. These are potentially responsible for the observed transition in density cross sections and profiles.

Fluctuations are strong on both inboard and outboard density gradients, suggesting drift wave activity. Though fluctuations peak on the outboard side of the plasma column, fluctuations on the inboard side are also abundant. Some fluctuations also change frequency with the magnetic field similarly to the prediction of linear drift wave theory: compare Figures 7 and 2, noting the plots have reversed axes. The absolute frequencies predicted and observed do not match, but the dependence of the frequency on magnetic field does match: in both simulation and experiment, the frequency increases by a factor of approximately 3/2 while the magnetic field doubles. Drift and interchange instabilities probably act in the ETPD. How they interact is yet unknown.

The fluctuation profiles in Figures 4 and 5 might also suggest a reduction in transport with increased neutral pressure. Fluctuations in the plasma column could drive plasma outward. If these occur in the center of the plasma column, the density profile may not be greatly effected. If these fluctuations occur near the edges, however, they could elongate the plasma column. The location of high- and low-frequency fluctuations move inward toward the center of the plasma column with increased neutral pressure. This may help explain the transition in density profile from wide to narrow.

Increasing fluctuation energy with higher pressure may be somehow involved with the transition in density profile. The maximum energy in both high- and low-frequency fluctuations increases with neutral pressure. Why this occurs is unknown but could provide another link to transport. As the neutral pressure increases, fluctuation energy increases but the density profile narrows. If these are connected, we might conclude fluctuations decrease transport toward the outboard side.

The change in relative amplitude of high- and low-frequency fluctuations indicates a change in the dominant fluctuation frequencies. At 1.1 mTorr, the low-frequency fluctuations dominate, and the density profile is broad. At 1.7 mTorr, the high-frequency fluctuations dominate, and the density profile is narrow. More data at different pressures could support or refute this observation.

The order of causation is unclear in this trend. Perhaps the several changes in fluctuations cause the density profile to change, or perhaps the change in profile causes the fluctuations to change. In the former case, we might conclude that fluctuation-driven transport causes the observed transition in density profile.

The phase shown in Figure /refmoving/reference isat cross-phase does not reveal simple mode structure in the low frequency fluctuations. Perhaps more structure would be visible in higher frequency ranges or some pattern would be evident with more data from cases of different pressure.

We clearly observe changes in the relative density cross sections with neutral-fill pressure. More in-depth analyses may reveal the proposed connection between cross-field transport and the transition in density profiles, as well as providing more details about the instabilities driving any transport.